Residual based *a posteriori* error estimates for MITC plate elements

Jarkko Niiranen
Department of Civil and Structural Engineering
Aalto University School of Engineering, Finland

in collaboration with

Lourenço Beirão da Veiga
Department of Mathematics
University of Milan, Italy

Rolf Stenberg
Institute of Mathematics and Systems Analysis
Aalto University School of Science, Finland

Contents

Contents

Introduction

- Bending of a thin plane structure occupied by

$$\mathcal{P} = \Omega \times (-\frac{t}{2}, \frac{t}{2}),$$

— with $\Omega \subset \mathbb{R}^2$ denoting the midsurface of the plate $\mathcal{P}$ and

— $t \ll \operatorname{diam}(\Omega)$ denoting the thickness of the plate.

- The material of the plate is assumed to be

— linearly elastic (defined by the generalized Hooke's law)

— homogeneous (independent of the coordinates x, y, z)

— isotropic (independent of the orientation).

- The transverse normal stress is assumed to vanish:

$$\sigma_{zz} = 0.$$

Variational formulation — Reissner–Mindlin

Let the deflection w and the rotation $\boldsymbol{\beta}$ belong to the spaces

$$W = \{v \in H^1(\Omega) \mid v = 0 \text{ on } \Gamma_{\mathrm{C_H}} \cup \Gamma_{\mathrm{C_S}} \cup \Gamma_{\mathrm{S_H}} \cup \Gamma_{\mathrm{S_S}}\},$$

$$\boldsymbol{V} = \{\boldsymbol{\eta} \in [H^1(\Omega)]^2 \mid \boldsymbol{\eta} \cdot \boldsymbol{n} = 0 \text{ on } \Gamma_{\mathrm{C_H}} \cup \Gamma_{\mathrm{C_S}},\ \boldsymbol{\eta} \cdot \boldsymbol{\tau} = 0 \text{ on } \Gamma_{\mathrm{C_H}} \cup \Gamma_{\mathrm{S_H}}\}.$$

Variational problem. *For the loading $f \in H^{-1}(\Omega)$, find $w \in W$ and $\boldsymbol{\beta} \in \boldsymbol{V}$ such that*

$$(\boldsymbol{E}\boldsymbol{\varepsilon}(\boldsymbol{\beta}), \boldsymbol{\varepsilon}(\boldsymbol{\eta})) + \frac{1}{t^2}(\nabla w - \boldsymbol{\beta}, \nabla v - \boldsymbol{\eta}) = (f, v) \quad \forall (v, \boldsymbol{\eta}) \in W \times \boldsymbol{V},$$

where the elasticity tensor $\boldsymbol{E}$ is defined as

$$\boldsymbol{E}\boldsymbol{\varepsilon} = \frac{\mathsf{E}}{12(1+\nu)}\left(\boldsymbol{\varepsilon} + \frac{\nu}{1-\nu}\operatorname{tr}(\boldsymbol{\varepsilon})\boldsymbol{I}\right) \quad \forall \boldsymbol{\varepsilon} \in \mathbb{R}^{2\times 2},$$

with the symmetric gradient, strain tensor $\boldsymbol{\varepsilon}$, Young's modulus E and the Poisson ratio ν.

Contents

MITC finite element methods

For a triangular MITC family, the discrete spaces for the deflection and the rotation are defined for $k \geq 2$ as

$$W_h = \{v \in W \mid v_{|K} \in P_k(K) \ \ \forall K \in \mathcal{C}_h\},$$

$$\boldsymbol{V}_h = \{\boldsymbol{\eta} \in \boldsymbol{V} \mid \boldsymbol{\eta}_{|K} \in [P_k(K)]^2 \oplus [B_{k+1}(K)]^2 \ \ \forall K \in \mathcal{C}_h\},$$

with the "bubble space" for the rotation

$$B_{k+1}(K) = \{b = b_3 p \mid p \in \tilde{P}_{k-2}(K),\ b_3 \in P_3(K),\ b_{3|E} = 0 \ \ \forall E \subset \partial K\}.$$

Finite element method. *(MITC: Bathe, Brezzi and Fortin 1989 etc.) Find $w_h \in W_h \subset W$ and $\boldsymbol{\beta}_h \in \boldsymbol{V}_h \subset \boldsymbol{V}$ such that*

$$(\boldsymbol{E}\boldsymbol{\varepsilon}(\boldsymbol{\beta}_h), \boldsymbol{\varepsilon}(\boldsymbol{\eta})) + \frac{1}{t^2}(\boldsymbol{R}_h(\nabla w_h - \boldsymbol{\beta}_h), \boldsymbol{R}_h(\nabla v - \boldsymbol{\eta})) = (f, v) \ \ \forall (v, \boldsymbol{\eta}) \in W_h \times \boldsymbol{V}_h,$$

where the reduction operator $\boldsymbol{R}_h : [H^1(\Omega)]^2 \to \boldsymbol{Q}_h$ *maps the shear force*

$$\boldsymbol{q}_h = \frac{1}{t^2}\boldsymbol{R}_h(\nabla w_h - \boldsymbol{\beta}_h) \in \boldsymbol{Q}_h \subset \boldsymbol{H}(\mathrm{rot}:\Omega)$$

into the rotated Raviart—Thomas polynomial space of order $k-1$*:*

$$\langle(\boldsymbol{R}_K\boldsymbol{\eta} - \boldsymbol{\eta})\cdot\boldsymbol{\tau}_E, p\rangle_E = 0 \quad \forall p \in P_{k-1}(E) \quad \forall E \subset \partial K,$$
$$(\boldsymbol{R}_K\boldsymbol{\eta} - \boldsymbol{\eta}, \boldsymbol{p})_K = 0 \quad \forall \boldsymbol{p} \in [P_{k-2}(K)]^2,$$

with $\boldsymbol{\tau}_E$ *denoting a unit tangent to* E*, while* $(\cdot,\cdot)_K$ *and* $\langle\cdot,\cdot\rangle_E$ *stand for the standard inner products in* $L^2(K)$ *and* $L^2(E)$*, respectively.*

Since it now holds that $\nabla W_h \subset \boldsymbol{Q}_h$, the shear force simplifies to

$$\boldsymbol{q}_h = \frac{1}{t^2}(\nabla w_h - \boldsymbol{R}_h\boldsymbol{\beta}_h).$$

Contents

Postprocessing

- The original deflection approximation is of order k:

$$w_{h|K} \in P_k(K).$$

- The postprocessed deflection approximation is of order $k+1$:

$$w^*_{h|K} \in P_{k+1}(K) = P_k(K) \oplus \widehat{W}(K) \oplus \overline{W}(K).$$

- New hierarchic degrees of freedom of order $k+1$, corresponding to the

  — element edges, by space $\widehat{W}(K)$, and

  — element interior, by space $\overline{W}(K)$,

  are added to the original approximation.

Postprocessing method

Determining the new – local – hierarchic degrees of freedom is based on the definition of the shear force:

$$\boldsymbol{q} = \frac{1}{t^2}(\nabla w - \boldsymbol{\beta}) \quad \text{or} \quad \nabla w = \boldsymbol{\beta} + t^2 \boldsymbol{q}.$$

Postprocessing method. *For each element K, find the local postprocessed deflection approximation $w^*_{h|K} \in P_{k+1}(K)$ such that*

$$I_h w_h^* = w_h \ \textit{ in the element } K,$$

$$\langle \nabla w_h^* \cdot \boldsymbol{\tau}_E, \nabla \hat{v} \cdot \boldsymbol{\tau}_E \rangle_E = \langle (\boldsymbol{\beta}_h + t^2 \boldsymbol{q}_h) \cdot \boldsymbol{\tau}_E, \nabla \hat{v} \cdot \boldsymbol{\tau}_E \rangle_E \ \ \forall \hat{v} \in \widehat{W}(K),$$

$$(\nabla w_h^*, \nabla \bar{v})_K = (\boldsymbol{\beta}_h + t^2 \boldsymbol{q}_h, \nabla \bar{v})_K \ \ \forall \bar{v} \in \overline{W}(K),$$

where $\widehat{W}(K)$ and $\overline{W}(K)$, respectively, correspond to the hierarchic edge and element (bubble) dofs of order $k+1$, while $I_h : H^s \to W_h$ denotes the corresponding hierarchic interpolation operator.

Convergence in the H^1-norm

Theorem. *(Lyly, Niiranen and Stenberg, 2007) Assuming a solution smooth enough, for the postprocessed deflection approximation w_h^* it holds that*

$$\|w - w_h^*\|_1 \le C(h+t)h^k\big(\|w\|_{k+1} + \|\boldsymbol{\beta}\|_{k+1} + \|\boldsymbol{q}\|_{k-1} + t\|\boldsymbol{q}\|_k\big).$$

- This gives an improvement of order $\mathcal{O}(h+t)$ to the original error estimate

$$\|w - w_h\|_1 \le Ch^k\big(\|w\|_{k+1} + \|\boldsymbol{\beta}\|_{k+1} + \|\boldsymbol{q}\|_{k-1} + t\|\boldsymbol{q}\|_k\big).$$

- Furthermore, according to the computational results, a corresponding accuracy improvement holds in the L^2-norm as well.

A new *a priori* error estimate

- Next, we define a mesh dependent norm coupling the deflection and the rotation as follows:

$$|||(v,\boldsymbol{\eta})|||^2 = ||\boldsymbol{\eta}||_1^2 + |(v,\boldsymbol{\eta})|_h^2,$$

$$|(v,\boldsymbol{\eta})|_h^2 = \sum_{K\in\mathcal{T}_h} \frac{1}{t^2+h_K^2}||\nabla v - \boldsymbol{\eta}||_{0,K}^2.$$

- This norm is stronger than the corresponding H^1-norms and it will be used for the *a posteriori* error analysis below as well.

Proposition. *Assuming a solution smooth enough, it holds that*

$$|||(w-w_h^*,\boldsymbol{\beta}-\boldsymbol{\beta}_h)||| \leq Ch^k\big(||w||_{k+2} + ||\boldsymbol{\beta}||_{k+1} + ||\boldsymbol{q}||_{k-1} + t||\boldsymbol{q}||_k\big).$$

Contents

A posteriori error estimates

We use the following notation as usual:

— $[\![\cdot]\!]$ for jumps (and traces),

— h_E and h_K for the edge length and the element diameter.

Internal error indicators

For all the elements K in the mesh $\mathcal{T}_h$,

$$\tilde{\eta}_K^2 = h_K^2(h_K^2 + t^2)||f + \operatorname{div} \boldsymbol{q}_h||_{0,K}^2 + h_K^2||\mathbf{div}\, \boldsymbol{m}(\boldsymbol{\beta}_h) + \boldsymbol{q}_h||_{0,K}^2,$$

and for all the internal edges $E \in \mathcal{I}_h$,

$$\eta_E^2 = h_E(h_E^2 + t^2)||[\![\boldsymbol{q}_h \cdot \boldsymbol{n}]\!]||_{0,E}^2 + h_E||[\![\boldsymbol{m}(\boldsymbol{\beta}_h)\boldsymbol{n}]\!]||_{0,E}^2,$$

with the moment tensor $\boldsymbol{m}(\boldsymbol{\eta}) = \boldsymbol{E}\boldsymbol{\varepsilon}(\boldsymbol{\eta})$.

Inconsistency error indicators

Due to the reduction $\boldsymbol{R}_h$ and postprocessing, we define the additional indicators: For the original MITC methods,

$$(\sigma_K)^2 = ||\mathrm{rot}\,(\boldsymbol{I} - \boldsymbol{R}_h)\boldsymbol{\beta}_h||_{0,K}^2 + ||(\boldsymbol{I} - \boldsymbol{R}_h)\boldsymbol{\beta}_h||_{0,K}^2$$
$$=: (\sigma'_K)^2 + (\sigma^0_K)^2,$$

while for the postprocessed MITC methods,

$$(\sigma_K)^2 = (\sigma'_K)^2 + (\sigma^*_K)^2,$$

$$(\sigma^*_K)^2 = \frac{t^4}{t^2 + h_K^2}||\boldsymbol{q}_h^* - \boldsymbol{q}_h||_{0,K}^2 = \frac{1}{t^2 + h_K^2}||(\boldsymbol{R}_h - \boldsymbol{I})\boldsymbol{\beta}_h - \nabla w_h^d||_{0,K}^2,$$

recalling the definitions $w_h^* = w_h + w_h^d$ and

$$\boldsymbol{q}_h = \frac{1}{t^2}(\nabla w_h - \boldsymbol{R}_h\boldsymbol{\beta}_h), \quad \boldsymbol{q}_h^* = \frac{1}{t^2}(\nabla w_h^* - \boldsymbol{\beta}_h).$$

Boundary error indicators

- The boundary of the plate is divided into
  - hard and soft clamped,
  - hard and soft simply supported,
  - and free parts:

$$\Gamma = (\Gamma_{\mathrm{C_H}} \cup \Gamma_{\mathrm{C_S}}) \cup (\Gamma_{\mathrm{S_H}} \cup \Gamma_{\mathrm{S_S}}) \cup \Gamma_{\mathrm{F}} \ .$$

- For boundary edges on $\Gamma_{\mathrm{C_S}}$, $\Gamma_{\mathrm{S_H}}$, $\Gamma_{\mathrm{S_S}}$ and Γ_{F}, respectively,

$$\begin{aligned}
\eta^2_{E,\mathrm{C_S}} &= h_E ||\boldsymbol{\tau} \cdot \boldsymbol{m}(\boldsymbol{\beta}_h)\boldsymbol{n}||^2_{0,E}, \\
\eta^2_{E,\mathrm{S_H}} &= h_E ||\boldsymbol{n} \cdot \boldsymbol{m}(\boldsymbol{\beta}_h)\boldsymbol{n}||^2_{0,E}, \\
\eta^2_{E,\mathrm{S_S}} &= h_E ||\boldsymbol{m}(\boldsymbol{\beta}_h)\boldsymbol{n}||^2_{0,E}, \\
\eta^2_{E,\mathrm{F}} &= h_E ||\boldsymbol{m}(\boldsymbol{\beta}_h)\boldsymbol{n}||^2_{0,E} + h_E(h_E^2 + t^2)||\boldsymbol{q}_h \cdot \boldsymbol{n}||^2_{0,E},
\end{aligned}$$

  measuring the fulfillment of natural boundary conditions.

Error indicators — local and global

- For any element $K \in \mathcal{T}_h$, the local error indicator is defined as

$$\eta_K = \Big(\tilde{\eta}_K^2 + \frac{1}{2} \sum_{E \in I(K)} \eta_E^2 + \sigma_K^2$$
$$+ \sum_{E \in C_{\mathrm{S}}(K)} \eta_{E,\mathrm{C_S}}^2 + \sum_{E \in S_{\mathrm{H}}(K)} \eta_{E,\mathrm{S_H}}^2 + \sum_{E \in S_{\mathrm{S}}(K)} \eta_{E,\mathrm{S_S}}^2 + \sum_{E \in F(K)} \eta_{E,\mathrm{F}}^2 \Big)^{1/2}$$

with the notation

— $I(K)$ for the set of internal edges of K,

— $C_{\mathrm{S}}(K)$, $S_{\mathrm{H}}(K)$, $S_{\mathrm{S}}(K)$ and $F(K)$, for the sets of boundary edges of K on $\Gamma_{\mathrm{C_S}}$, $\Gamma_{\mathrm{S_H}}$, $\Gamma_{\mathrm{S_S}}$ and Γ_{F}, respectively.

- The global error estimator is finally defined as

$$\eta_h = \Big(\sum_{K \in \mathcal{T}_h} \eta_K^2 \Big)^{1/2}.$$

Upper bound — Reliability

Theorem. *Reliability: There exists a positive constant C such that*

$$|||(w - w_h^*, \boldsymbol{\beta} - \boldsymbol{\beta}_h)|||^2 + t^2 ||\boldsymbol{q} - \boldsymbol{q}_h||_0^2 \\ + ||\boldsymbol{q} - \boldsymbol{q}_h||_{\boldsymbol{V}'}^2 + t^4 ||\mathrm{rot}\,(\boldsymbol{q} - \boldsymbol{q}_h)||_0^2 \le C\,\eta_h^2.$$

Lower bound — Efficiency

Theorem. *Efficiency: There exists a positive constant C such that*

$$\eta_h^2 \le C \Big(|||(w - w_h^*, \boldsymbol{\beta} - \boldsymbol{\beta}_h)|||^2 + t^2 ||\boldsymbol{q} - \boldsymbol{q}_h||_0^2 \\ + ||\boldsymbol{q} - \boldsymbol{q}_h||_{\boldsymbol{V}'}^2 + t^4 ||\mathrm{rot}\,(\boldsymbol{q} - \boldsymbol{q}_h)||_0^2 + \mathrm{osc}(f)^2 \Big).$$

Efficiency is proved by standard arguments, whereas reliability needs more technicalities (taking inspiration from the work of Carstensen and Hu, 2008).

Contents

Benchmark results from adaptive computations

- We have implemented
  - — the lowest order MITC7 element ($k = 2$)
  - — with the postprocessing and error indicators
  - — in the open-source finite element software *Elmer* developed by CSC – the Finnish IT Center for Science.
- For adaptive mesh refinements, the software provides
  - — error balancing strategy and
  - — complete remeshing for triangular meshes.

Semi-infinite plate — boundary layers

- We consider the plate domain $\Omega = \{(x, y) \in \mathbb{R}^2 \mid y > 0\}$:
  — Poisson ratio $\nu = 0.3$, shear modulus $G = \frac{1}{2(1+\nu)}$
  — thickness $t = 0.01$
  — loading $f = G^{-1} \cos x$.
- On the boundary $\Gamma_x = \{(x, y) \in \mathbb{R}^2 \mid y = 0\}$, two different types of boundary conditions are imposed:
  — hard simply supported (**no** boundary layer) or
  — free (**strong** boundary layer).
- We discretize the domain $\overline{D} = [0, \pi/2] \times [0, 3\pi/2]$ with nonhomogenous Dirichlet boundary conditions matching the exact solution on the boundary part $\partial D \setminus \Gamma_x$.

Hard simply supported boundary — regular solution
Convergence — uniform vs. adaptive

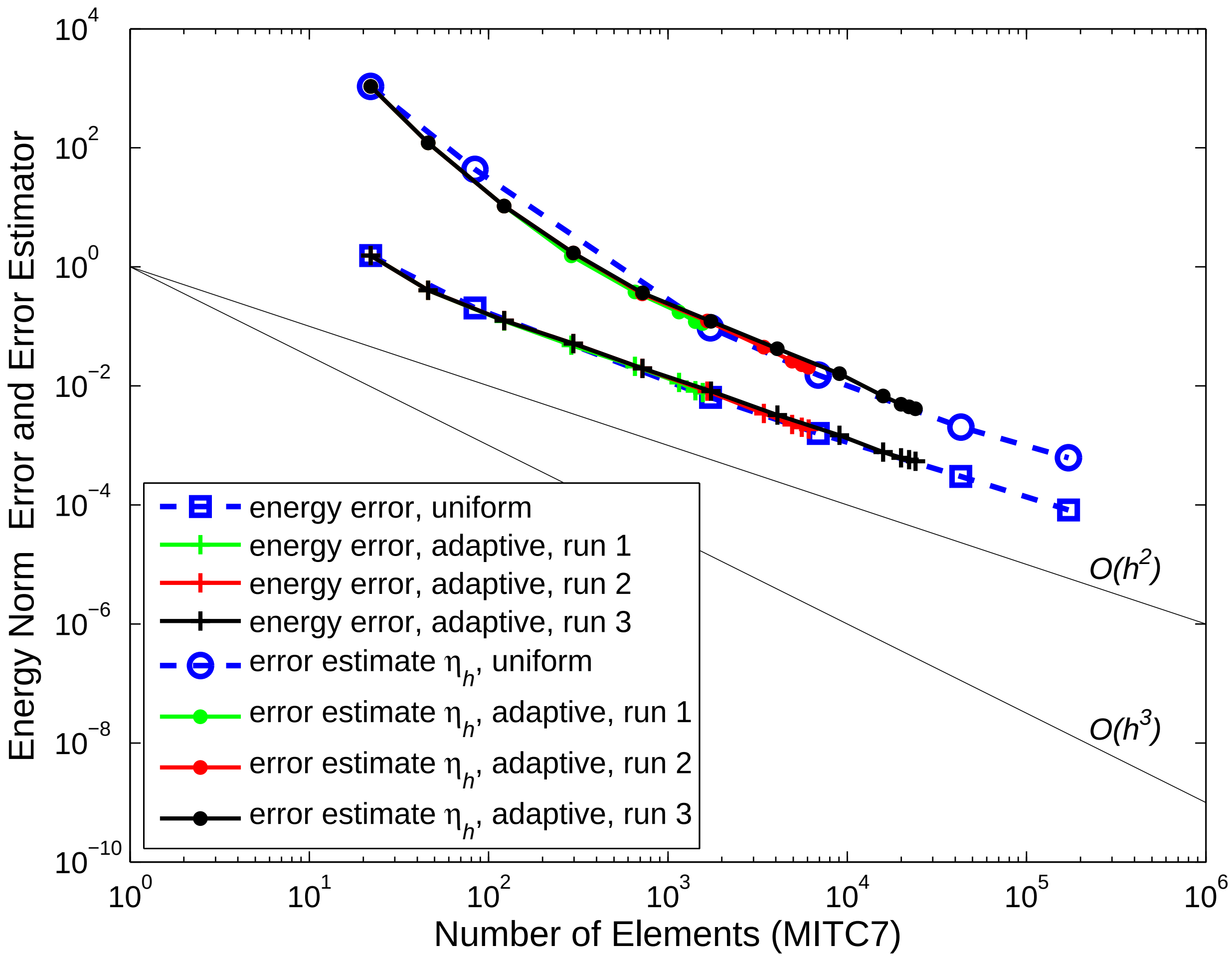

Hard simply supported boundary — regular solution Convergence — contributions of the error indicators

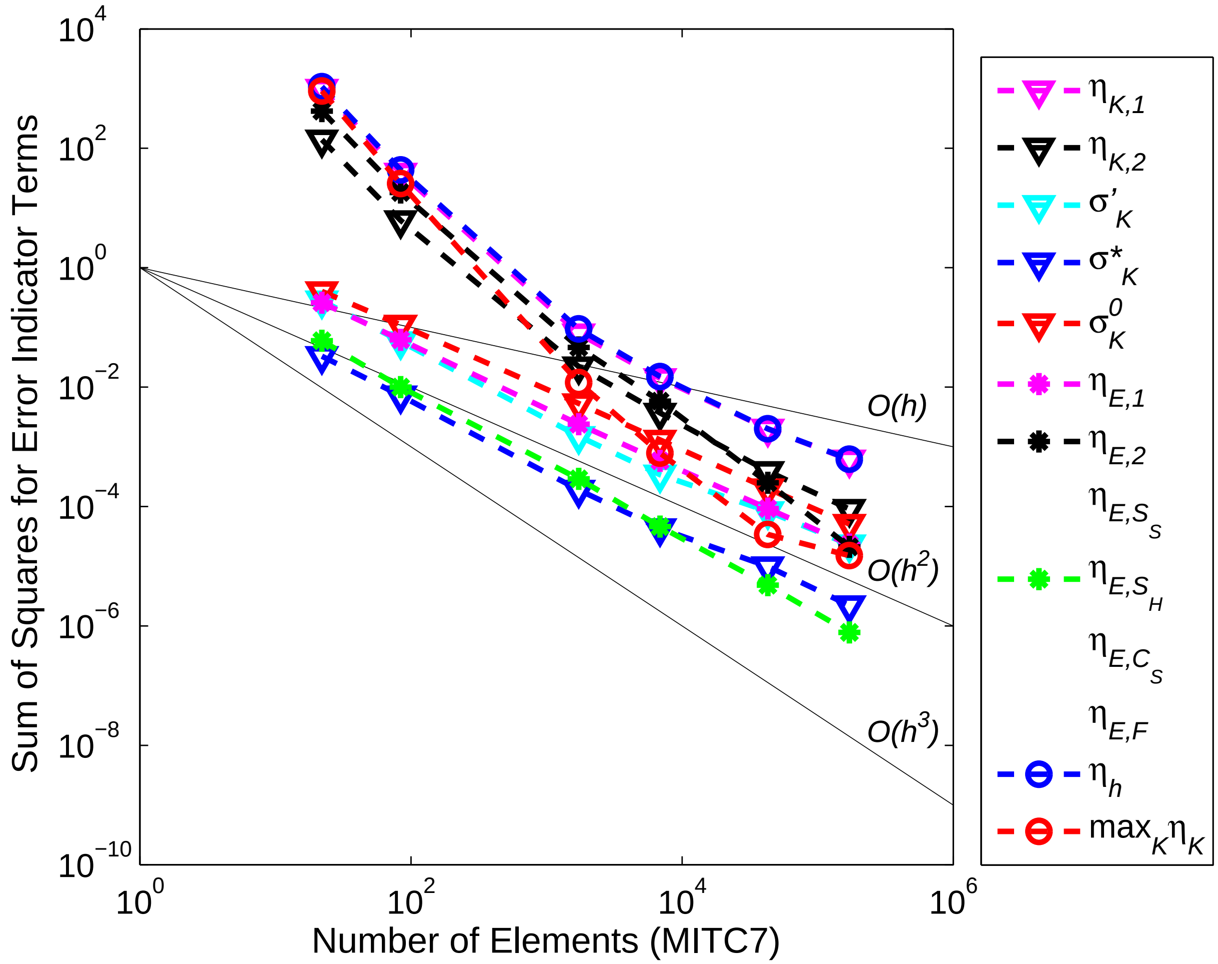

Free boundary — boundary layer
Adaptively refined meshes

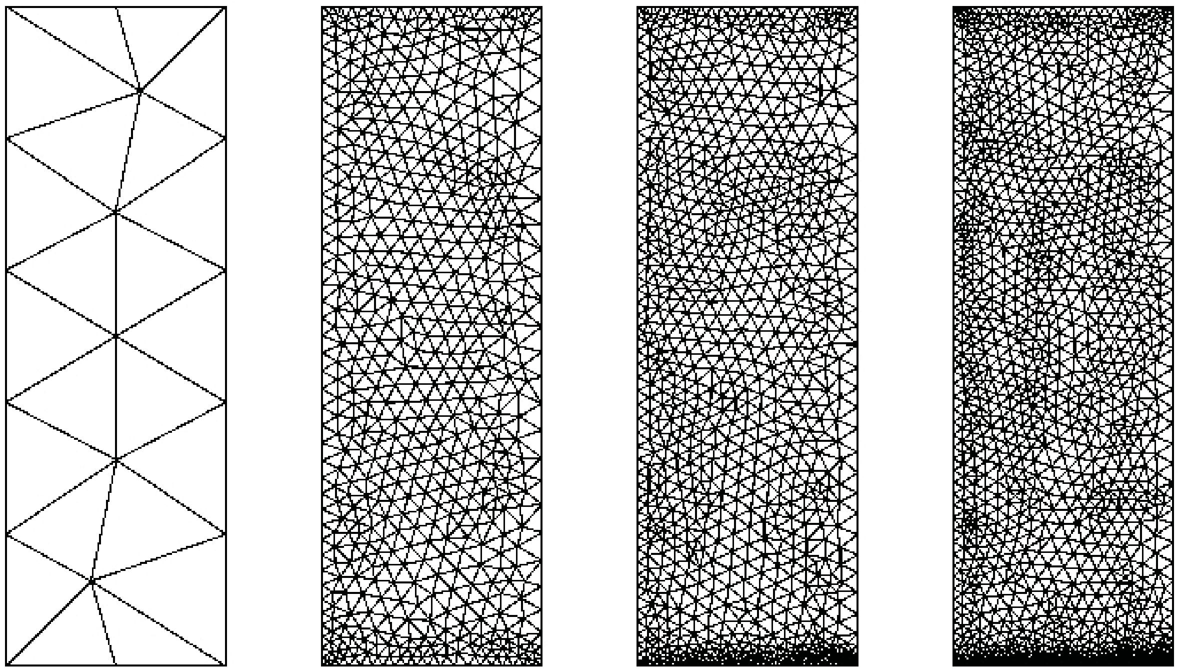

Figure 1: Semi-infite domain, free boundary, $t = 0.01$: Meshes for the **steps 1, 6, 8 and 12** (the last step) of an adaptive run with $N = 22$, 1160, 1856 and 3558, respectively.

Free boundary — boundary layer
Convergence — uniform vs. adaptive

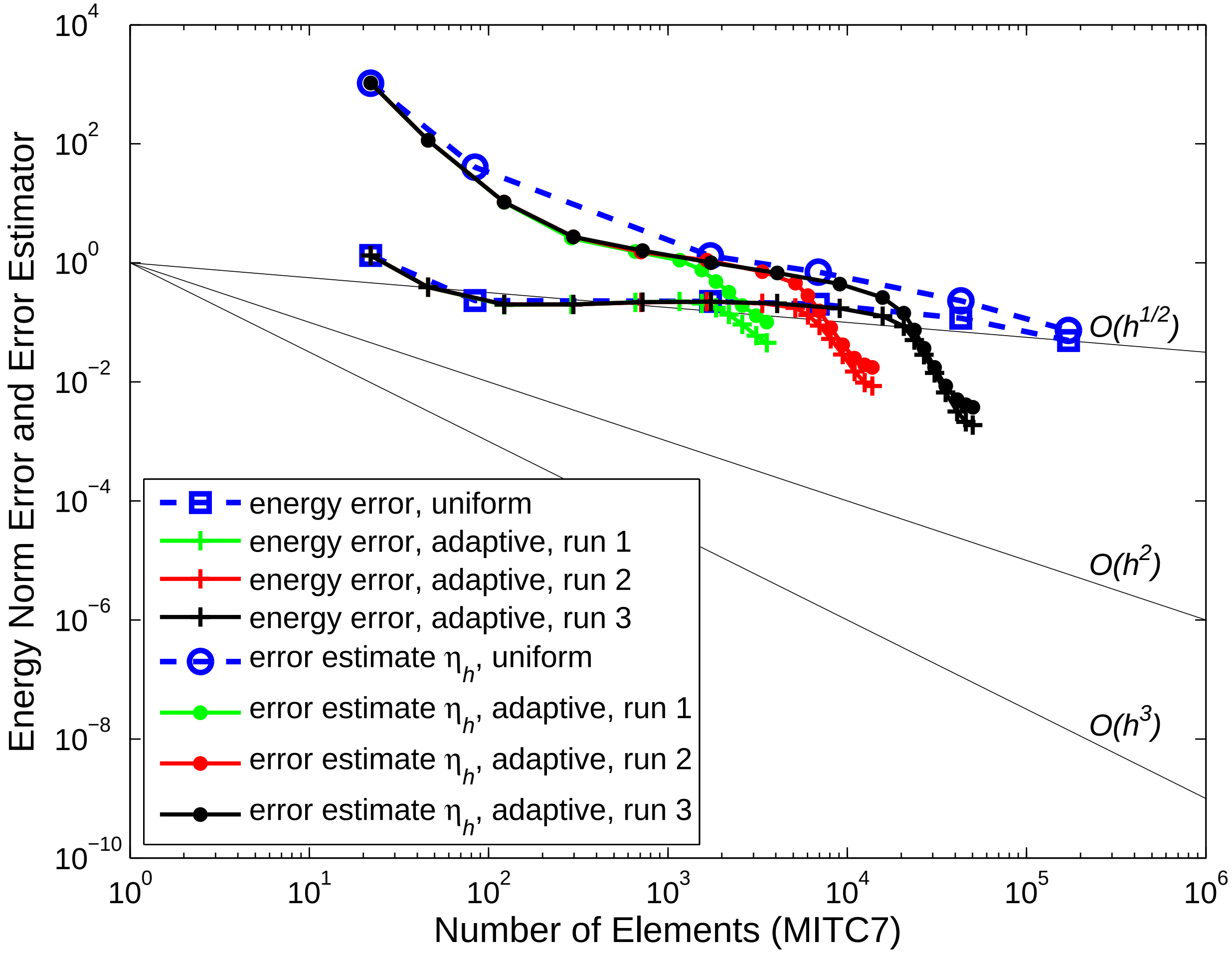

Free boundary — boundary layer
Convergence — contributions of the error indicators

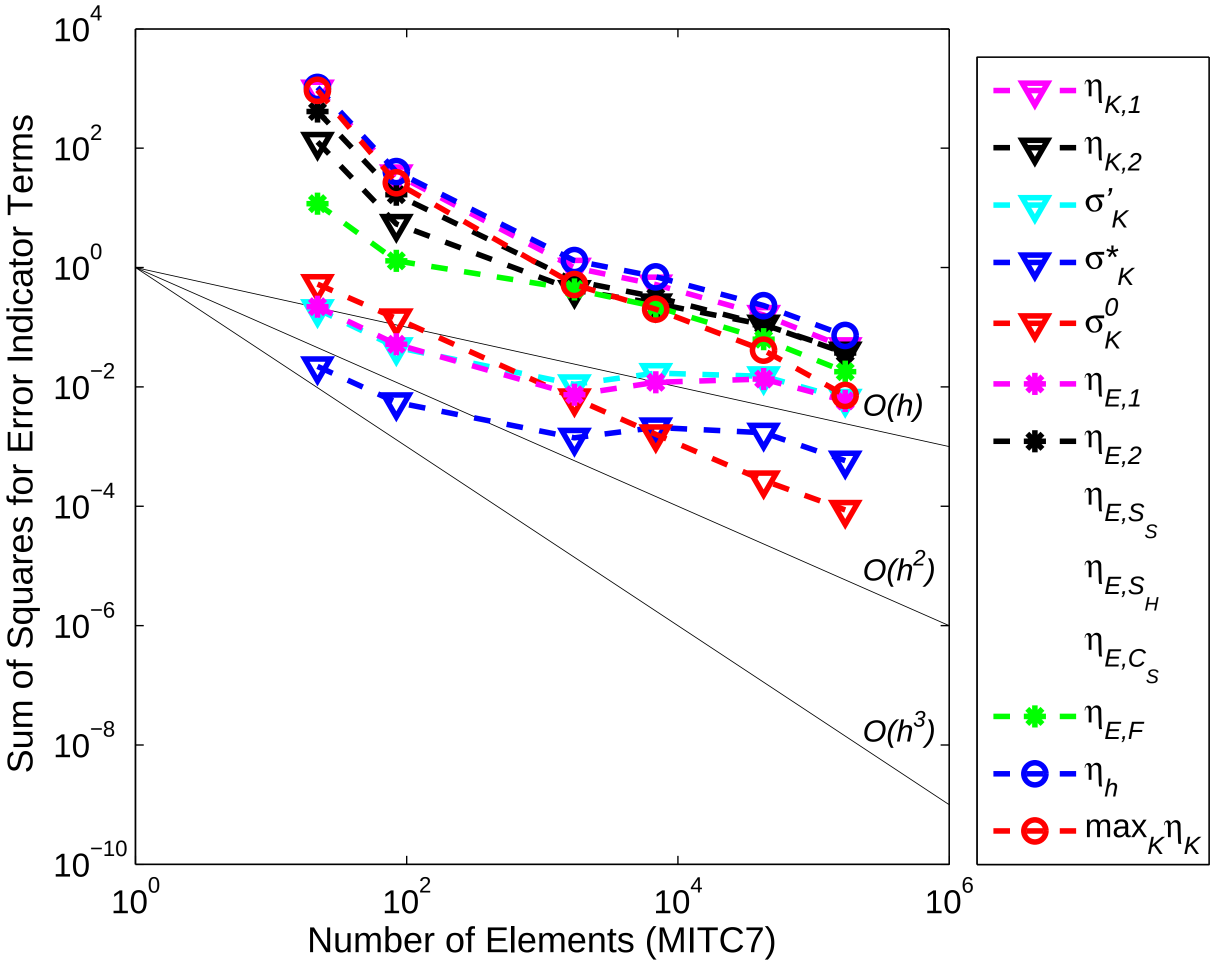

Free boundary — boundary layer
Mesh refinements — the first ... the final

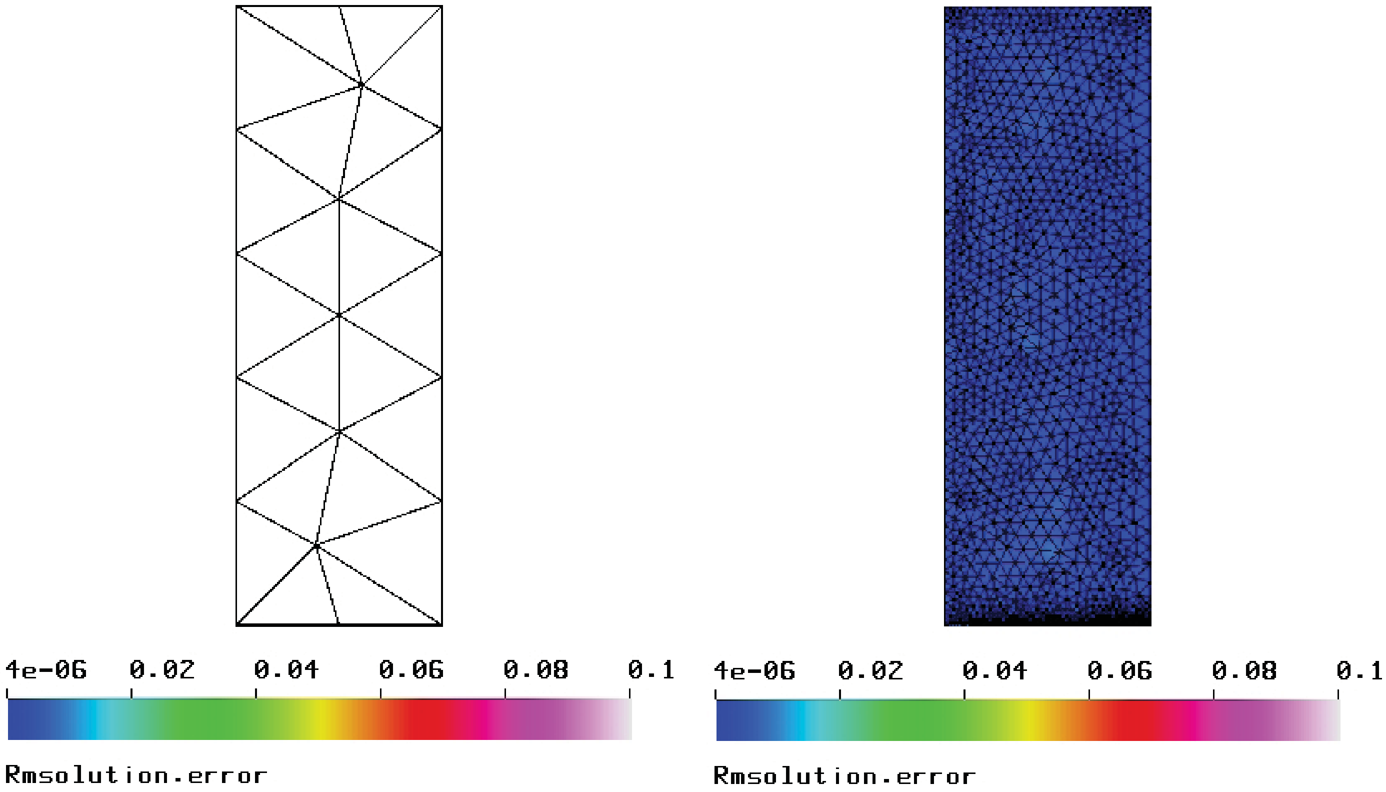

Free boundary — boundary layer
Mesh refinements — ... a closer look on the final

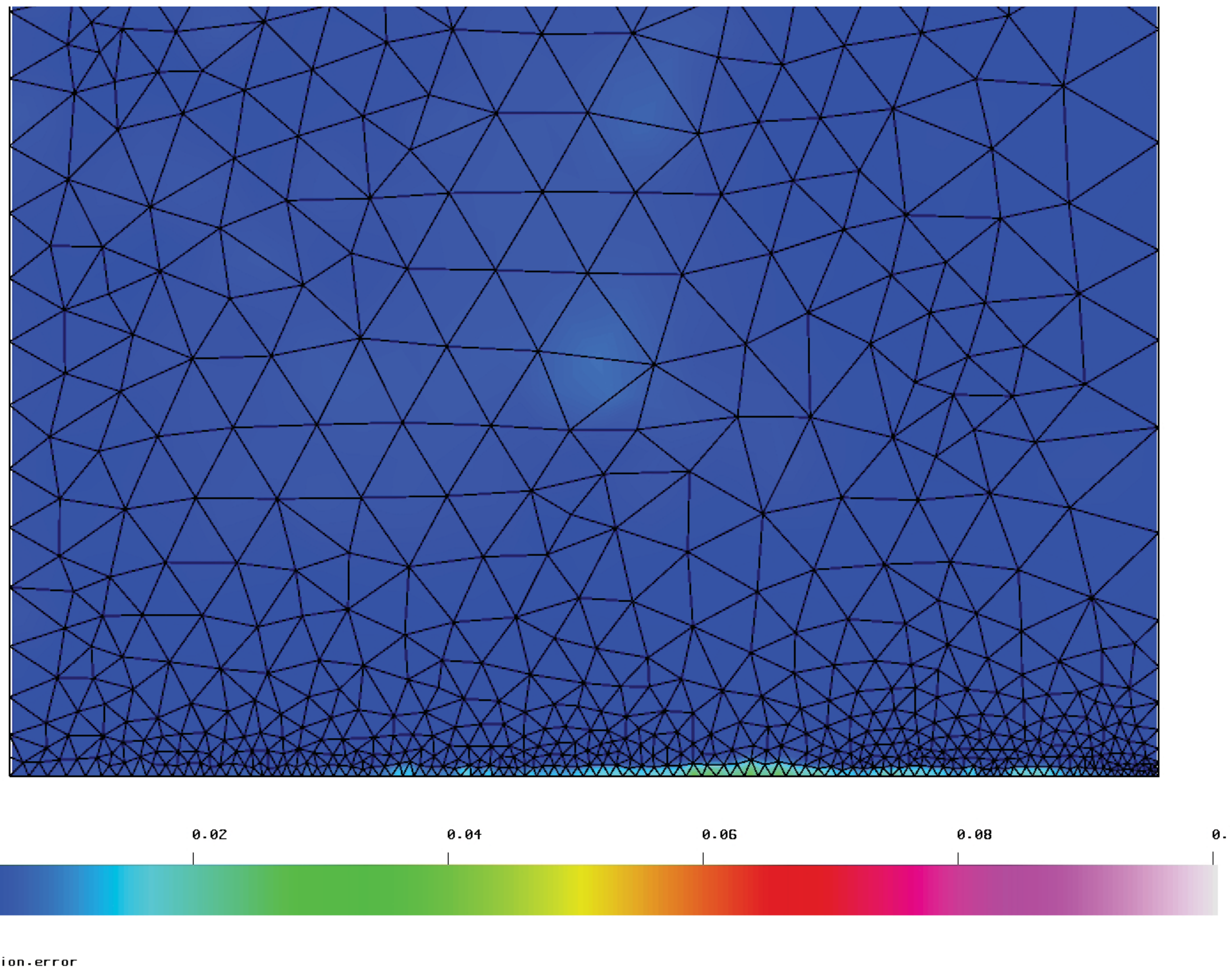

Non-convex domains
— corner singularities and boundary layers

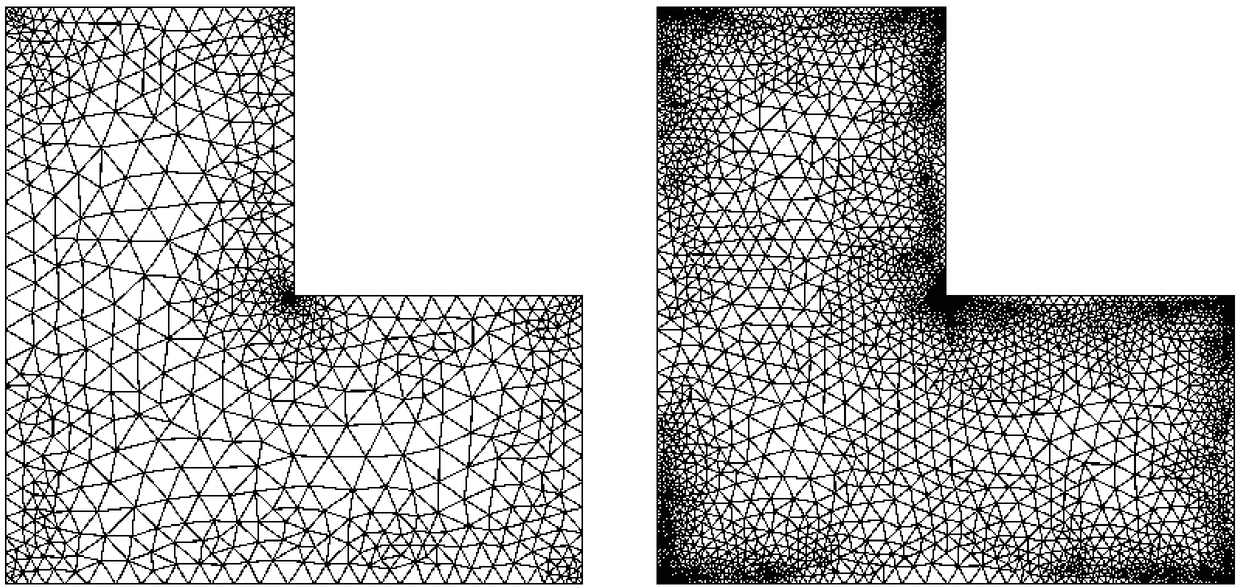

Figure 2: L-shaped domains, $t = 0.01$: Meshes for the final **steps 12 and 20** of adaptive runs with $N = 1301$ and $N = 6208$, respectively, for **soft clamped** (left) vs. **soft simply supported** (right) boundaries

Non-convex domains
Convergence — uniform vs. adaptive

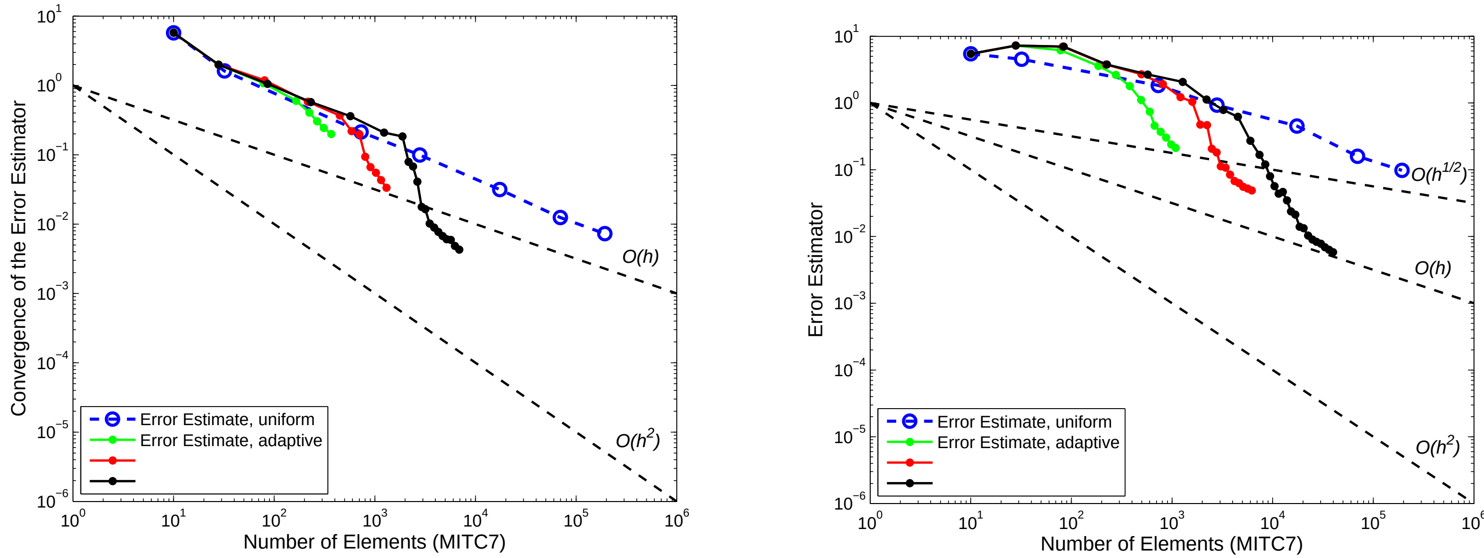

Figure 3: L-shaped domains, $t = 0.01$: **soft clamped** (left) and **soft simply supported** (right) boundaries.

Contents

Conclusions and discussion — advantages

- Reliability: computable (non-guaranteed due to C) global upper bound for the error.
- Efficiency: computable (non-guaranteed due to C) local lower bound.
- Robustness: C independent of the mesh size, data and the solution.
- Small computational costs: local postprocessing and indicators.
- Element independent: applicaple for a wide range of MITC elements.

Conclusions and discussion — disadvantages

- Methodology: residual based error estimates in the energy norm only
  — no estimates for other quantities of interest.
- Method and problem dependence: applicaple for MITC methods for Reissner–Mindlin plates only
  — the methodology and techniques are general, however.
- Validity: proved and tested only for static problems with transversal loading and isotropic, homogeneous, linearly elastic material
  — so far.

References

[1] M. Lyly and J. Niiranen, R. Stenberg, Superconvergence and postprocessing of MITC plate elements; *Computer Methods in Applied Mechanics and Engineering*, 196, 3110–3126 (2007).

[2] C. Carstensen and J. Hu, A posteriori error analysis for conforming MITC elements for Reissner–Mindlin plates; *Mathematics of Computation*, 77, 611–632 (2008).

[3] L. Beirão da Veiga, J. Niiranen and R. Stenberg. *A posteriori* error analysis for the postprocessed MITC plate elements; *submitted for publication* (2011).